

Magnetic Critical Phenomena in the Stellar Corona

Tzihong Chiueh, Carrie J. L. Lai, Huan-Hsin Li, and Wean-Shun Tsay
*Institute of Astronomy and Department of Physics, National Central University,
Chung-Li, Taiwan 320, R.O.C.*
(Received August 18, 1995)

A new continuous-state cellular automata model continuous-state is proposed to describe the non-linear dynamical processes of flaring stellar magnetic fields. The large-scale electric current density is identified as being the only order parameter for this model when the system approaches phase transitions. At the critical state, various measurable quantities are found to exhibit scaling relations. Among them, the frequency distribution of the flare energy obtained from this model is found to be in fair agreement with the currently available x-ray data.

PACS. 97.10.Ex – Stellar atmospheres.

PACS. 97.10.Ld – Magnetic and electric fields; polarization of starlight.

PACS. 97.30.Nr – Flare stars.

I. Introduction

Over the past years it has been observed that, in the Sun [1] as well as in magnetically active stars [2], intermittent bursts of energy exhibit behaviors reminiscent of those observed in critical phenomena. Specifically, the probability $f(E)$ (or frequency) for the release of a certain energy E often obeys a universal scaling relation. In the case of the Sun, such a scaling relation is observed in the hard x-rays and extends over several decades in energy [1]. In the case of magnetically active stars, however, the scaling relation has been detected over a smaller range due to the faintness of the distant stars [2]. It is nevertheless believed that the Sun, as well as magnetically active stars, obey a similar universal scaling law: $f(E) \propto E^{-\alpha}$, with $\alpha \sim 1.4$.

The Sun is a typical star, for which the surface structures can be observationally resolved in great detail. By contrast, magnetically active stars are so distant that they appear as point sources. Based on the belief that magnetic activity in the solar atmosphere should represent a scaled-down version of what is happening on a magnetically active star, in the following we keep in mind the better-understood solar magnetic activity as a typical working example.

The solar corona is filled with electrically highly conducting hot ($> 10^6 K$) plasmas and magnetic fields; the energy density of the latter can be two orders of magnitude higher than that of the former, and above the active region the coronal magnetic fields are estimated to be as high as 100 Gauss [3]. Flares and micro-flares are manifestations of the bursting release of energy. Although the detailed mechanisms of the solar (micro-) flares are not yet

well-understood, for many years the re-structuring of the photospheric and chromospheric magnetic fields prior to and after the flares has led investigators to believe that it is the reconnection of the magnetic fields in the corona that underlies the physical mechanisms causing the bursts. Recent observations of the Yohkoh z-ray satellite have, for the first time, revealed a great many details of such dynamical processes, reinforcing the belief in support of the important role of the coronal magnetic fields and universality behavior [4] in the flares.

Reconnection of the equilibrium magnetic field lines in an electrically highly conducting plasma, known as the linear tearing instability, begins at low amplitudes [5]. When entering the nonlinear regime the reconnected field lines often consist of a mixture of chaotic small-scale features and a large-scale ordered field superimposed with turbulent flows. Reconnection, together with the random convection from the flow, makes the magnetic field appear diffusive, much like the turbulent diffusion of a passive scalar in fluid turbulence. Diffusion of the magnetic fields yields a decrease in the magnetic energy, converting a fraction of the original magnetic energy into heat, a part of which is in the form of photons and the other in the form of the thermal energy of electrons and ions.

Sudden flare bursts reveal that magnetic reconnection can be turned on vigorously within a short period of time, but remains quiescent most of the time [6]. The rarity of larger energy-releasing events suggests that the magnetic system requires a longer time to store a larger amount of energy [7]. On one hand, these phenomena are highly nonlinear, and on the other, self-regulating. Combining these, one is naturally led to the speculation that these phenomena resemble those exhibiting "Self-Organized Criticality (SOC)" [8], such as with the avalanches. Much like the avalanches, in the solar atmosphere the energy is injected into the coronal fields through photospheric flow motion. When locally satisfying a threshold condition, a tearing instability sets in, triggering turbulent diffusion, releasing the excess magnetic energy and forcing the field to reach a lower energy state. The fact that the system has the capacity to store a finite amount of energy before release makes it able to exhibit the SOC.

Most recently, a series of pioneering papers have appeared in the literature, advocating the novel idea of SOC for explaining the solar flares [9,10]. This approach abandons the traditional one that looks into the details of the reconnection processes and turns to an understanding of the statistical behaviour of the flares. This approach also has the advantage of making more direct contact with the currently available x-ray data [10].

Unfortunately, these papers have erroneously adopted a representation of the magnetic field \mathbf{B} that does not obey the divergence-free condition, $\nabla \cdot \mathbf{B} = 0$. Violation of the divergence-free condition for the magnetic field may be fatal since this condition forces the deposited random vector field $\delta\mathbf{B}(\mathbf{x})$ to be strongly correlated with other vector fields in the neighboring sites $\delta\mathbf{B}(\mathbf{x} \pm \delta\mathbf{x})$. Without the divergence-free constraint, the $\delta\mathbf{B}$ on each site can be regarded as completely independent. Despite the acclaimed agreement with the observations by the authors of these papers, the lack of strong correlation among the vector fields in adjacent sites makes one suspect the validity of such a claim. It is the purpose of this paper to examine the critical phenomena of magnetic reconnection in the solar corona in the simplest possible way, capturing the essential features of the magnetic fields and their dynamics.

II. Quasi-two dimensional turbulent reconnection model

Since a one-dimensional magnetic field can be regarded as a scalar, the simplest nontrivial vector field is a two-dimensional field. However, another consideration, to be elucidated in the next paragraph, reveals that a strictly two-dimensional field misses some important features, and a slight extension to a quasi-two dimensional configuration is needed. In this report, we shall adopt this simplest, but reasonable, model as the test bed for a series of investigations to follow in the future.

In a plasma that has a low thermal pressure compared with the magnetic pressure, *no* non-trivial two dimensional field, except for the potential field, is possible in equilibrium. As often adopted in the literature of Solar Physics, one must superimpose a strong, nearly uniform and nearly potential field in the third dimension to maintain the force balance during the quiescent states in the corona. The superimposed field can be taken to be perpendicular to the solar surfaces at the photosphere, and we shall call it the longitudinal field. (This field actually nearly follows the coronal potential field. With certain simplifications for this model the potential field can be regarded as a uniform field along the vertical direction. See Fig. 1 and its figure caption for details.) The existence of the longitudinal field allows the field lines to be connected to the photosphere, thereby extracting the fluid motion energy of the solar granulations to store it in the transverse field. It can be shown that the coronal current is associated mainly with the transverse field, and therefore the transverse field is the key component that gives rise to the released bursts of energy. Incorporation of the longitudinal field has thus no dynamical significance during the reconnection phase; it only serves to extract the granular motion energy in the slowly evolving energy injection phase.

In the slowly evolving quiescent state, energy is injected into the transverse field \mathbf{B}_2 through the relation [11,12]

$$\frac{\partial \mathbf{B}_2}{\partial t} \cdot \mathbf{t} \mathbf{V}_2 \cdot \nabla \mathbf{B}_2 - \mathbf{B}_2 \cdot \nabla \mathbf{V}_2 = B_3 \frac{\partial \mathbf{V}_2}{\partial z}, \quad (1)$$

where the right-hand side is the source, \mathbf{V}_2 is the slow transverse motion of the field lines in a perfect conductor, B_3 is the longitudinal (z) component of the magnetic field and ∇ is the two-dimensional gradient, operator transverse to the z -direction. Note that the right-hand side of Eq. (1) contains the essential physics of field line bending, which, together with the boundary condition at the photosphere permits the transport of the photospheric motion energy into the transverse field \mathbf{B}_2 via low-frequency Alfvén waves. After the onset of MHD instabilities, fast dynamics is turned on. While the longitudinal field remains little changed, the transverse field is basically controlled by two-dimensional dynamics, where the Reduced MHD approximation applies [11,12,13]. When the fluid motion becomes sufficiently turbulent, one may model the dynamical equation of the field lines as a diffusion-like equation, mimicking turbulent diffusion:

$$\frac{\partial \mathbf{B}_2}{\partial t} + \nabla \times (D \nabla \times \mathbf{B}_2) = B_3 \frac{\partial \mathbf{V}_2}{\partial z}, \quad (2)$$

where D , determined by the local turbulent velocity, is the spatial-dependent turbulent diffusion coefficient. During the rapid turbulent phase, the right-hand side source is small

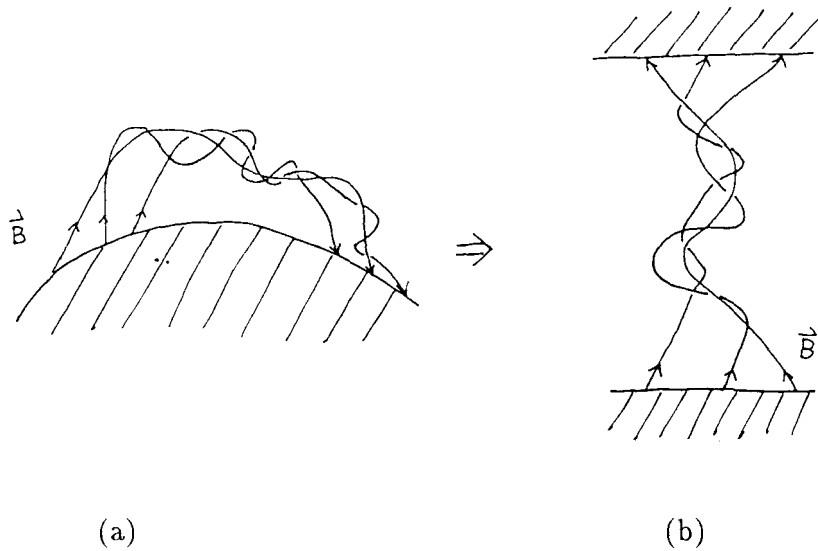


FIG. 1. (a) A sector of typical magnetic field configurations above the photosphere in the solar corona. (b) The simplified version of the coronal fields for our model, which retains the same field topology and connectivity in the photosphere as the one shown in (a). The shaded regions represent the photosphere.

compared with left-hand side turbulent diffusion and we may, for the sake of convenience, turn off the energy source until the local dissipation is completed and resume the slow energy injection dynamics described by Eq. (1).

The onset of turbulent reconnection begins with the tearing instability, which is generally controlled by the local electrical current density $\mathbf{j} = j\hat{\mathbf{z}} = \nabla \times \mathbf{B}_2$. Thus we shall assume that whenever the absolute value of the local current density exceeds some threshold value j_{max} turbulent reconnection is turned on and the dynamical evolution immediately switches from Eq. (1) to Eq. (2). The exact value of the turbulent diffusion coefficient D is irrelevant in this model as long as the rate of energy release is much greater than that of energy injection. Separation between the time scales of the energy release and injection allows one to assume that, once initiated, the magnetic reconnection must have been completed long before the next photospheric energy is available for injection into the corona.

Finally, the remaining issue to be considered is toward what configuration the locally reconnected fields are relaxed. Complete relaxation must exhaust all the available free energy, which vanishes when the current density \mathbf{j} vanishes. We shall therefore assume that the relaxed field should locally reach the lowest available energy state which has a zero current density, $\mathbf{j} = 0$.

The major improvement in this work, compared with the previous ones, is that the condition $\nabla \cdot \mathbf{B} = 0$ is obeyed. Quasi-two dimensional fields have been shown to be well approximated by the Reduced MHD equations, where the transverse magnetic field can be described by a scalar function ψ :

$$\mathbf{B}_2 = -\hat{\mathbf{z}} \times \nabla \psi, \quad (3)$$

and the longitudinal field B_z , to the leading order, as a constant [11,12,13]. The scalar function ψ is understood as the transverse magnetic flux; energy injection from photospheric motion can be regarded as an injection of random magnetic flux into the corona. Thus, we are essentially dealing with a random scalar field instead of the random vector field adopted in the previous works. The former can be made to automatically satisfying the $\nabla \cdot \mathbf{B} = 0$ condition; whereas the latter can not.

III. Continuous-state cellular automata model

The preceding considerations allow us to construct a cellular automata (CA) model of continuous states, which mimics the evolution of the coronal fields. Conventional CA models assume a finite number of discrete states at each lattice site [14]. However, in our model the value of the vector field \mathbf{B} is not discrete but continuous for the following two reasons. First, we are interested in the continuous dynamics of diffusion describable by a partial differential equation, and second, the magnetic field must satisfy the divergence free condition, which involves a differential operator on \mathbf{B} , making it impossible for the value of \mathbf{B} to be discrete.

III-1. Energy injection

Energy injection by random photospheric motion into the corona is a slower process than energy release. We may let the injection processes be represented by the injection of one unit of either positive or negative magnetic flux $\delta\psi$ into a randomly selected site at every time step. (We also investigate the cases where the amount of flux injection at every time step is not a fixed quantity but a random variable.) In fact, to better describe the coronal fields, we decompose the magnetic fields into a static large-scale field and dynamical small-scale fields, with the former being associated with the very slow large-scale photospheric shear motions and the latter with the granular motions. Therefore the energy injection consists of two parts: the nearly static large-scale background field that carries a uniform current and the flux injection into a randomly selected site at every time step by the small-scale granular motion.

In this work, we let the background field \mathbf{B}_0 be initially given by:

$$\mathbf{B}_0 = -\hat{y}J_0x, \quad (4)$$

or the background magnetic flux by

$$\psi_0 = 0.5J_0x^2, \quad (5)$$

in the domain between $0 \leq x \leq \mathbf{L}$, where J_0 is the uniform background current.

Evolution of the coronal fields begins by injecting a unit of equally probable positive or negative magnetic flux $\delta\psi$ into a random site at every time step. This procedure continues until at any site a certain criterion on the local current strength is satisfied. When this is so, the nonlinear diffusion of the magnetic fields is turned on so as to release the local magnetic stress. Soon after the relaxation is completed, flux injection is then re-initiated.

We set the boundary condition in the z -direction in such a way that the magnetic fields at the boundaries ($x = 0, \mathbf{L}$) are always kept the same during the evolution. The

boundaries in the y -direction are taken to be periodic. This boundary condition in \mathbf{x} is important in that, in addition to the energy injection from the random granular motion, it also provides gross energy input into the system, mimicking the energy injection from the large-scale shear motion. Actually, a major fraction of the energy dissipated during the relaxation is actually fed by such large-scale shear motion. It turns out that the average background current density J_0 , measuring the amount of local free energy stored in the large-scale, in effect serves as the order parameter indicating how far the system is from the criticality.

111-2. Nonlinear diffusion

When the absolute value of the current density at any given site exceeds a threshold ($|j(\mathbf{x})| \geq j_{th}$), the tearing instability sets in and turbulent diffusion is immediately turned on. The dynamics switches to that described by Eq. (2). We let

$$D(\mathbf{x}) = D_0 > 0, \quad (6)$$

for sites where the local current densities exceed the threshold, and

$$D(\mathbf{x}) = 0 \quad (6')$$

otherwise. The exact value of the diffusion constant D_0 is not relevant as long as the turbulent relaxation is much faster than the energy injection. The binary nature of the diffusion coefficient $D(\mathbf{x})$ suggests that such diffusion be highly nonlinear.

Practically, we are dealing with the evolution of the flux function ψ . The current density j is calculated from ψ through the relation: $j = -\nabla^2 \psi$. Once the turbulent diffusion at a particular site is turned on, the local flux ψ is set to a value that equals the averaged flux of the surrounding sites at the previous time step. In other words, for a two-dimensional square lattice, the new local flux is set to the average of the 4 old fluxes surrounding this site. This procedure effectively sets the local current density equal to zero, and also has the advantage that the dynamics can always be advanced in time with fewer operations, a forward advancing numerical scheme. It can be easily shown that such a diffusion operation always reduces the local magnetic stress B^2 , thereby releasing the magnetic energy.

Diminution of the local current density by the aforementioned operation may sometimes enhance the current densities of the neighboring sites, making them exceed the threshold and triggering further nonlinear diffusion at time steps thereafter. That is, nonlinear diffusion of this nature has the capability to propagate and spread once a single site is ignited. When the system reaches a critical state, the probability of the spreading size obeys a scaling relation, as does that of the energy dissipation. As we have previously stated, J_0 is the order parameter and there exists a critical value, J_c at which the critical state is reached. (The exact value of J_c can be determined by the value of the threshold current j_{th} and the size of injected flux that we have arbitrarily chosen; however the ratio J_c/j_{th} will be found independent of the value of j_{th} as long as the size of injected flux is sufficiently small.) Below this critical current, large-scale chained-diffusion is absent; above the critical current, the system becomes supercritical, abundantly populating with ever-increasing

large-sized chained-diffusion, and occasionally a single diffusion event may even continue forever without stopping.

In the next section, we will investigate various critical scaling relations of such a dynamical system; in particular, it is of interest to us to find out how much these scaling relations depend on the value of j_{th} , a quantity that can not be universal because it must depend very sensitively on the geometry and shape of the field lines in order for the tearing modes to be triggered.

IV. Numerical results

In each simulation run, we let J_0 be a given order parameter. Shown in Fig. (2) is the log-log plot of the histogram (or distribution function) of the released energy for a typical subcritical J_0 . Large events do occur but only very rarely. They do not show any power-law scaling. As the value of J_0 increases, one finds that the power-law relation becomes more pronounced. Shown in Fig. (3) is the histogram of the released energy at criticality, where $J_0 = J_c$. The distribution function obeys

$$f(E) \sim E^{-\alpha}, \quad (7)$$

with $\alpha \approx 1.2$. This value of α remains rather robust for a wide range of the threshold current, j_{th} , and for situations where the injected flux at every time step varies in size. We find that as long as the injected flux size is sufficiently small, the ratio J_0/j_{th} becomes independent of the value of j_{th} , and our results yield $J_c/j_{th} \rightarrow 0.6$.

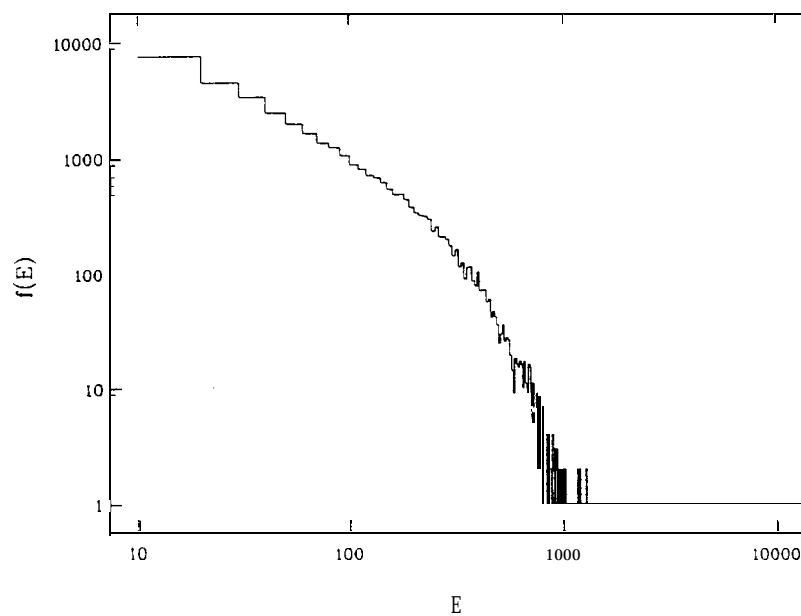


FIG. 2. The distribution function $f(E)$ for a value of J_0 that is subcritical.

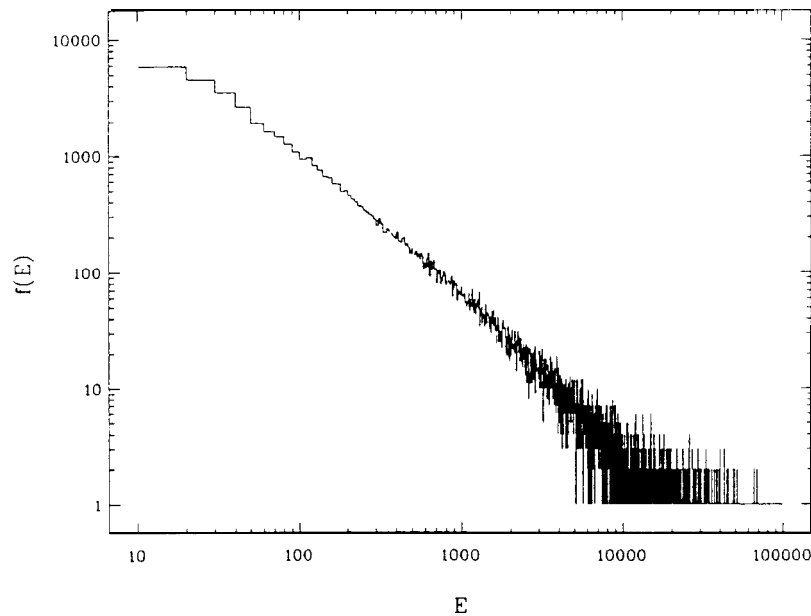


FIG. 3. The distribution function $f(E)$ for a case that has critical J_0 .

We have not extended our study to the effect of finite system size L . In the simulations, L has been taken to be 200 grid length, which is much larger than the grid size. In this regime, the results should approach the infinite size limit.

It is of interest to examine the waiting time $T_w(E)$ of an event that releases a certain energy E after a previous event of the same size. Plotted in Fig. (4) is the distribution of E against $T_w(E)$, in 10^6 time steps, at the critical state. The plot clearly shows that the interval between larger events is, on the average, longer. To analyze the distribution in a more quantitative way, we plot the distribution of events in three bands cutting across Fig. (4). We define the line $\ln(T(E)) + 0.8\ln(E) = b$, and the three bands are defined as in between $9 < b < 12$, $12 < b < 15$ and $15 < b < 18$, which we shall call the A, B and C bands, respectively. Plotted in Figs. (5) are the distribution of the events against the quantity $0.8 \ln(T(E)) - \ln(E) (\equiv a)$ in the A, B and C bands, respectively. Except for the amplitudes, the distributions $h(a)$ for the three appear similar in the locations of the peaks and in their widths as well as in their skewed tails. We may empirically conclude that the distribution of events in the $(E, T(E))$ phase space, as shown in Fig. (4), can be approximated by

$$F(a, b) = g(b)h(a). \quad (8)$$

The function $h(a)$ appears to be the superposition of a Gaussian and a tail. The tail is skewed toward the negative side of a , as is clearly shown in Fig. (4) where sparsely scattered points extend into the upper left corner. The function $g(b)$ decreases monotonically with b , and has no trivially recognizable functional form.

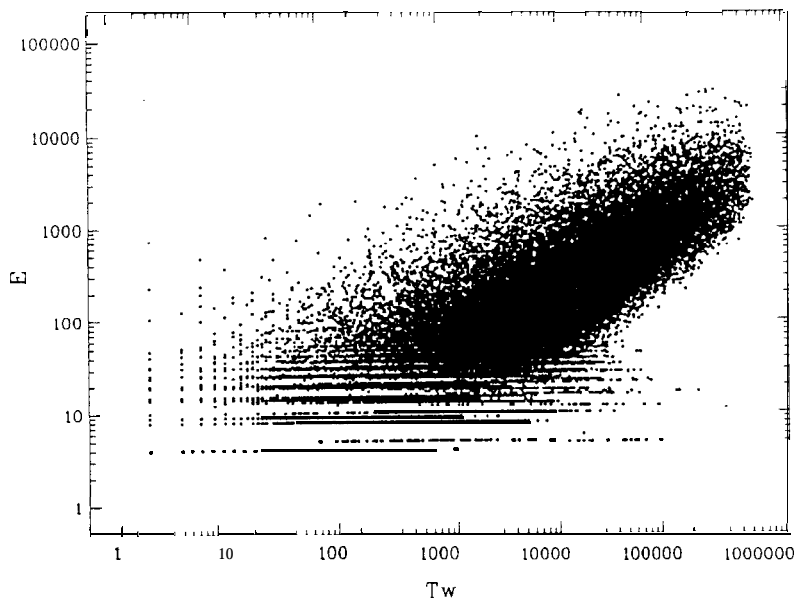


FIG. 4. The distribution of the events in the $E-T_w$ phase space when the current J_0 is critical. Each dot represents an event.

V. Conclusions

We have investigated the critical phenomena of the stellar coronal magnetic fields using a model of continuous-state cellular automata. The actual energy injection is due to the photospheric large-scale shear motion and small-scale random motion, and is described by the magnetic induction equation, Eq. (1). The actual energy dissipation is due to a sudden onset of turbulent diffusion, described by Eq. (2). The dynamics of our cellular automata model is capable of capturing the above two pieces of physics, and producing genuine critical phenomena. We find that the large-scale current resembles the order parameter of critical phenomena in Thermodynamics. In particular, we find that the distribution function, $f(E)$, of the released energy during the bursts obeys a scaling relation with E (cf., Eq. (7)). Additionally, we may also determine the approximate functional relation between the waiting time T_w and the released energy E .

Insofar as the actual observations of the solar z-rays are concerned, we find that our numerically determined relation of $f(E) (\propto E^{-1.2})$ is in fair agreement with the z-ray data: $f(E) \propto E^{-\alpha}$, with $\alpha \approx 1.4$. In view of the simplicity of our model, such agreement is rather encouraging. Much room remains for further refinement of our model to better compare with the observations. One major extension of the present model entails the inclusion of the possible transverse current that manifests the interaction of coronal loops running in opposite directions. Such a refinement requires additional scalar functions to describe the evolution of the three components of the magnetic field. A refinement of this kind is non-trivial and investigation in this direction is underway.

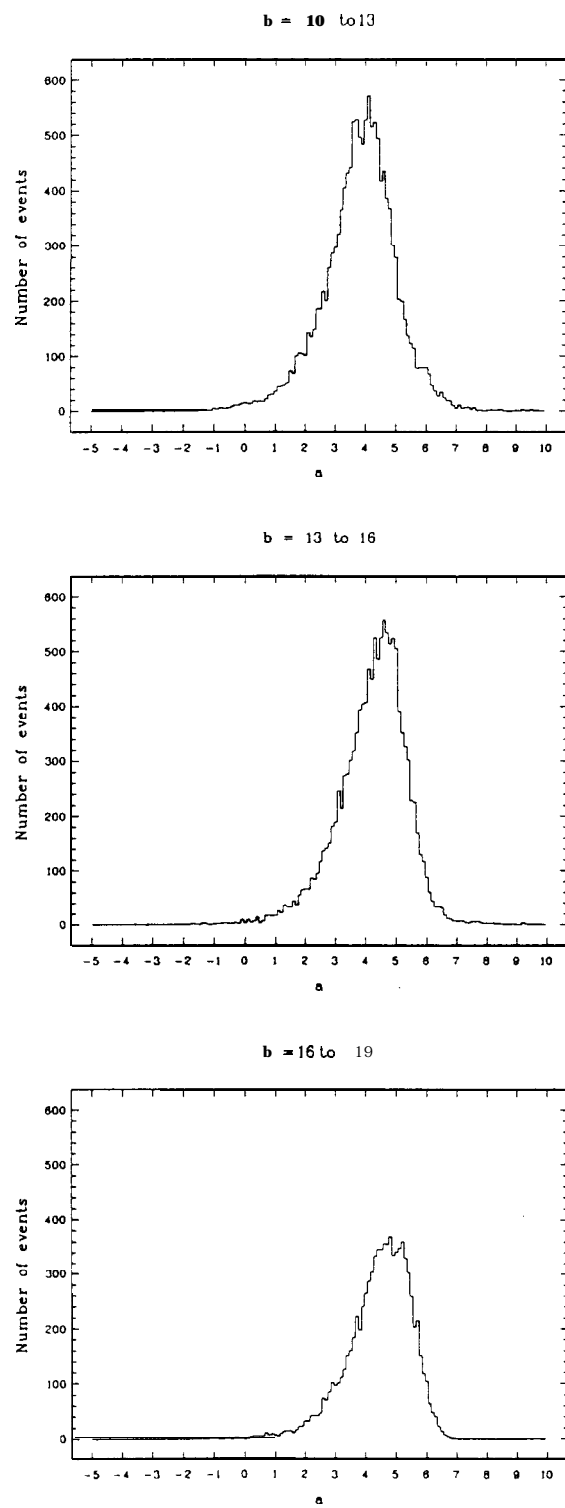


FIG. 5. Plots of the integrated number of events as a function of a for three bands of b in Fig. (4), where a and b are defined in the text.

Acknowledgements

This work was supported by the National Science Council of Taiwan under the grants: NSC 84-2612-M008-005 and NSC 84-2112-M008-017.

References

- [1] B. R. Dennis, *Solar Phys.* 100, 465 (1985).
- [2] N. I. Shakhovskaya, *Solar Phys.* 121, 375 (1989).
- [3] E. N. **Parker**, *Cosmic Magnetic Fields* (Oxford Univ. Press: Oxford 1979).
- [4] T. Shimizu, *Pub. Astron. Soc. Jap.* 47, 251 (1995).
- [5] H. P. Furth, J. Killeen, and M. N. Rosenbluth, *Phys. Fluids* 6, 459 (1963).
- [6] P. Foukal, *Solar Astrophysics* (Wiley: New York 1990).
- [7] T. Chiueh and E. G. Zweibel, *Astrophys. J.* 338, 1158 (1989).
- [8] P. Bak, C. Tang, and K. Wiesenfeld, *Phys. Rev. Letts.* 59, 381 (1987).
- [9] E. T. Lu and R. J. Hamilton, *Astrophys. J.* **380**, L89 (1991).
- [10] E. T. Lu, R. J. Hamilton, J. M. McTiernan, and I. R. Bromund, *Astrophys. J.* 541, 841 (1993).
- [11] H. R. Strauss, *Phys Fluids* 19, 134 (1976).
- [12] T. Chiueh and E. G. Zweibel, *Astrophys. J.* **317**, 900 (1987).
- [13] E. N. Parker, *Astrophys. J.* 341, 389 (1993).
- [14] N. H. Packard and S. Wolfram, *J. Stat. Phys.* 38, 901 (1985).